IEEE Access
Multidisciplinary | Rapid Review | Open Access Journal

Received June 21, 2020, accepted July 13, 2020, date of publication July 27, 2020, date of current version August 7, 2020.

Digital Object Identifier 10.1109/ACCESS.2020.3012125

Crop and Weed Leaf Area Index Mapping Using Multi-Source Remote and Proximal Sensing

MUHAMMAD HAMZA ASAD AND ABDUL BAIS, (Senior Member, IEEE)
Faculty of Engineering and Applied Science, University of Regina, Regina, SK S4S 0A2, Canada

Corresponding author: Abdul Bais (abdul.bais@uregina.ca)

This work was supported in part by the Natural Sciences and Engineering Research Council of Canada Alliance Grant entitled Ground Truth Validation of Crop Growth Cycle Using High Resolution Proximal and Remote Sensing with Phantom Ag Ltd., and Croptimistic Technology Inc., and in part by Mitacs Accelerate Grant entitled Weed Classification and Density Estimation for Variable Rate Herbicide Prescription.

ABSTRACT Site specific management rationalizes farm inputs and mitigate environmental impacts. Traditionally, low resolution satellite imagery and soil maps are employed for site specific decisions in large scale farms. However, these approaches are not good at sub-field level due to low spatial resolution. To overcome this problem, either manual scouting is employed or extensive high resolution data collection platforms are used. In both cases, the cost outweighs the expected returns. Consequently, variable rate applications are not preferred in large fields. Leaf Area Index (LAI) is a useful measure to monitor crop growth and health for site specific management. In this paper we propose an accurate and scalable process where multispectral remote sensing and proximal sensing data is used to estimate LAI. Crop LAI (CLAI) and Weed LAI (WLAI) are estimated from limited high resolution ground image samples using semantic segmentation. These limited LAIs are extended to the whole field using remote sensing and proximal sensing data. We find that LAIs are spatially related with Soil, Water and Topography (SWAT) maps and are field specific. With increasing weed population in the fields, correlation of WLAI with the SWAT zone increases. However, CLAI remains comparatively consistent across SWAT zones due to variable rate seeding and fertilizer application based on soil variance. Our results demonstrate that LAIs can be predicted accurately from limited high resolution ground imagery, satellite imagery, SWAT, and soil properties maps.

INDEX TERMS Leaf area index, machine learning, multispectral satellite imagery, site specific management, SWAT maps.

I. INTRODUCTION

Site Specific Management (SSM) is popular among small agricultural farm holdings. It increases farmer profitability by increasing yield and rationalizing farm inputs. It also mitigates the detrimental effects of agricultural practices on environment [1]. SSM is performed relatively easier by the farmers in smaller farms because they have access to every inch of the land. It helps them monitor crop health and deploy control measures. With the growing farm size, land and crop information is sparsely accessible, hampering informed decision making for SSM. Consequently, farmers use uniform rate inputs on larger fields. The farmers' decision of adopting SSM is largely determined by economic motives [2] which means that cost of data acquisition and processing should be lower than its potential benefits.

LAI is an important intrinsic physical property of vegetation, which is used for crop growth and health monitoring and help in SSM [3]. Traditionally, LAI is estimated using remote sensing based vegetation indices at field level [4], [5]. However, the spatial resolution of none of these vegetation indices is high enough to make LAI useful for SSM. It means that extensive ground truth validation is necessary to employ SSM. One option is to manually scout the fields and record both CLAI and WLAI and other crop affecting factors. The other option can be extensive acquisition of high resolution ground imagery and processing it through machine learning and deep learning techniques to extract useful information. Both options have their own problems. The former is costly, time consuming and have accessibility issues, and the latter has complexities of image acquisition and data handling.

The midway is to use limited high resolution ground imagery for estimation of CLAI and WLAI using deep learning based semantic segmentation techniques and then finding a scientific way to predict CLAI and WLAI for the whole field. In this paper we establish the relationship of LAIs and soil related causes of it. Soil, Water and Topography (SWAT) map categorizes land into 10 zones using soil

The associate editor coordinating the review of this manuscript and approving it for publication was Gerardo Di Martino.

properties like Electrical Conductivity (EC), Elevation (EV), Water Flow(WF), and water accumulation maps. We use SWAT zoning and other soil properties like EC, EV, and WF for establishing relationship between LAIs and soil properties. Once relationship is established, a function is mapped using Artificial Neural Network (ANN) between multispectral satellite imagery, soil properties, and LAIs extracted through ground imagery. The mapped function predicts the WLAI and CLAI for the rest of the field. In this paper, satellite imagery from Planet Lab RapidEye satellite are used. SWAT and soil properties maps are provided by CropPro Consulting [6]. We observe that WLAI extracted from high resolution ground imagery, is strongly related with SWAT zones. CLAI is more consistent across SWAT zones as soil related issues are addressed using variable rate application of seeding and fertilizer. The results also demonstrate that local variations estimated using limited high resolution ground imagery can be used to predict LAIs for the whole field with acceptable accuracies. The paper makes following novel contributions:

1) Estimating LAI using multi-source information.
2) Bifurcating LAI into CLAI and WLAI using semantic segmentation.
3) Correlational study to establish relationship between CLAI and WLAI with SWAT zones.
4) CLAI and WLAI estimation from high resolution ground imagery, soil related maps, and satellite imagery.

The remainder of the paper is organized as follows: Section II presents related work, Section III describes the methodology, Section IV is about result discussion, and Section V is conclusion and recommendations for future work.

II. RELATED WORK

LAI is vegetation leaf area per unit ground area. It is a fundamental biophysical method to judge crop growth and health. Breda categories LAI estimation methods into two categories: direct method and indirect method [7]. Direct method involves actual measurement of leaf area using leaf measurement tools. Indirect methods estimate LAI from reflectance based non-intrinsic vegetation indices that measure crop health, but does not quantify vegetation. The former method is costly, complex, and time consuming while the latter is economical and scalable thanks to satellite imagery [7]. Carlson *et al.* explore LAI relationship with Normalized Difference Vegetation Index (NDVI). They observe linear relationship between LAI and NDVI for lower values of LAI. At LAI threshold of 2-3, NDVI becomes less sensitive to LAI changes, which highlights limitation of NDVI in estimating LAI [8]. Viña *et al.* compare various indirect LAI estimation methods by acquiring data through close range spectrometer (6 *m* above canopy) and plane mounted hyper spectral spectrometer. Their results demonstrate that chlorophyll indices exhibit strong linear relationship for LAI [4]. Similarly, Dong *et al.* find strong relationship of red-edge and LAI [9].

Apart from various vegetation indices, spatial resolution of the sensors mounted on satellite or aerial platform determine the ultimate utility of the target variables. Landsat, Moderate Resolution Imaging Spectroradiometer, Thematic Mapper, Advanced Very High-Resolution Radiometer are widely employed for estimating yield, biomass, and LAI at very large scale as spatial resolution varies from 30 *m* to 1000 *m* [10]–[12]. These satellites have low spatial resolution making them unsuitable for sub-field SSM. Recently, high spatial and temporal resolution satellite imagery is made available from Planet Lab satellites like RapidEye. Shang *et al.* and Dong *et al.* use RapidEye based vegetation indices for LAI estimation and correlational study [9], [13]. To account for the crop structure, Hosseini *et al.* augment optical RapidEye data with Synthetic Aperture Radar data [14]. In addition to improvements in satellite data, various machine learning techniques are used to train LAI estimation models. Wang *et al.* use Support Vector Regression (SVR), random forest and ANN for modelling biomass [15]. Gahrouei *et al.* compare SVR and ANN for biomass and LAI estimation from vegetation indices extracted from canola, corn, and soya bean crops [16]. Guanter *et al.* use deep learning techniques on Unmanned Aerial Vehicle (UAV) imagery to accurately estimate LAI [17]. It shows that in-field LAI mapping is possible with scalability. Despite improving spatiotemporal resolution of remote sensing data, it still falls short of finding the soil related causes of LAI variations and bifurcating LAIs into CLAI and WLAI, which are crucial for variable rate SSM.

For variable rate SSM, two approaches are found in literature: map based SSM and sensor based SSM. Map based methods are offline, which process maps of interest back in office and construct variable rate prescription maps to feed in application equipment. In case of sensor based SSM, data is collected, processed and decision is made on equipment for adjusting the rate of application. Due to limitations of application equipment like on-site sensing, processing and implementing variable rate, offline map based methods are popular. In map based approaches, remotely sensed data acquired through UAV, aerial and satellite platforms are used to monitor crop growth and health. This information is used to identify homogenized management zones for variable rate applications [18]. Ess *et al.* use both remote sensing and proximal sensing to construct soil maps to manifest spatial variability of the field [19]. Variations of soil potential may result in varying nature of LAI in field. Ilyas *et al.* study effects of variations in ground elevations on LAI and biomass [20]. Organic content, moisture content and water flow patterns effect the LAI and yield of crops [21]. Similarly, distribution of weeds are linked with soil properties. It is found that distribution of weeds is patchy in nature. Soil properties, cropping year, type of weeds and adaptability character of weeds with changing conditions are some of the many factors that explain patchy distribution of weeds [22]. Soil properties like pH, chemical composition, texture and organic matter are correlated with weed density.

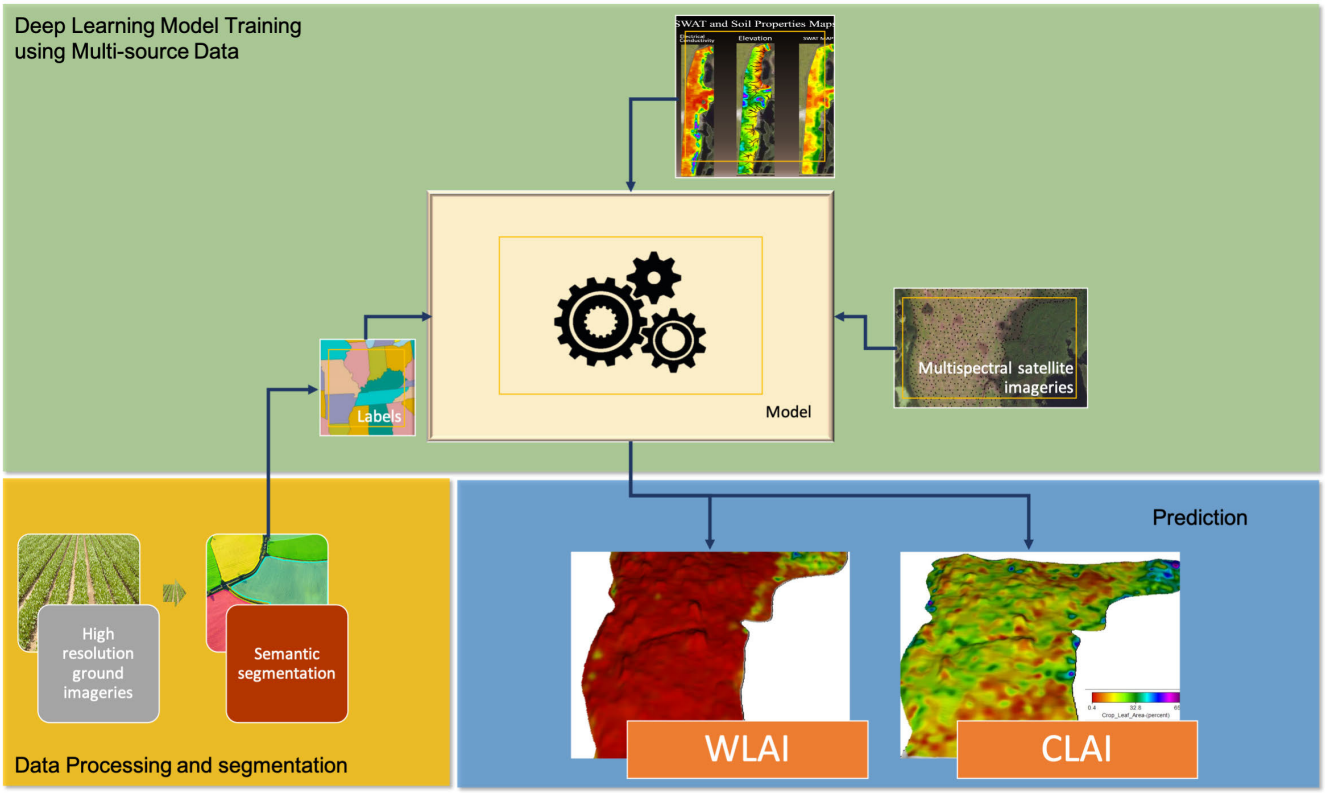

FIGURE 1. Crop Leaf Area Index (CLAI) and Weed Leaf Area Index (WLAI) estimation from remote sensing (satellite imagery) and proximal sensing (soil properties and high-resolution ground imagery) data using machine learning techniques.

Weed growth differs with change of environment [23], [24]. Metcalfe *et al.* employ variogram for studying spatial relationship between soil and weed count [25]. They also study variation of organic matter and moisture content in the field. Weed patches are present in the areas of high organic matter and moisture content because herbicides have been less effective in zones of high water and organic content [26]. Similarly, soil texture and soil pH variations are also related with weed density. Alkaline clay soils have more weed density as compared to sandy acidic soils [27], [28]. Korres *et al.* and Metcalfe *et al.*'s correlation studies demonstrate that there exist relationship between spatial distribution of different weeds and soil properties [29], [30]. The results of above-cited works demonstrate that crop and weed distribution relates with soil properties which suggests that soil data may be used in addition to satellite data for LAI estimation.

Despite all above-cited works, LAIs can not be used for SSM due to low spatial resolution [31]. To address this problem, alternate approach is to acquire high resolution ground imagery using ground moving platform or UAV and then process these images using machine learning and deep learning techniques [32], [33]. Convolutional neural networks are widely applied for weed detection, plant recognition, and land cover classification [34]. We have employed semantic segmentation techniques SegNet and U-NET for weed detection and density estimation in the oats, wheat, and canola fields [35], [36]. However, the cost is higher for data acquisition and handling as there is scarce internet infrastructure in rural areas and climatic conditions are not suitable with special reference to Canadian Prairies. We address this problem by acquiring limited number of representative high resolution images in a grid pattern using ground moving imaging platform like field sprayers, tractors, and quads. To the best of our knowledge, the method proposed in this paper to estimate CLAI and WLAI using limited high resolution ground imagery, satellite based vegetation indices, SWAT zoning, and soil maps is not used before.

III. METHODOLOGY

In this paper, the above-identified problem is addressed by combining multi-source remote sensing satellite data and proximal sensing soil data to estimate CLAI and WLAI. Ground truth CLAI and WLAI labels are calculated by segmenting high resolution geo-referenced ground imagery using deep learning based semantic segmentation. Relationship between LAIs and SWAT and soil properties maps is established. The fields showing LAIs' relationship with SWAT and soil properties are selected for training machine learning model in order to predict LAIs for the whole field. The flowchart in Fig. 1 explains all the steps involved. The following subsections provide the details.

A. GROUND IMAGERY

This study is conducted in collaboration with our industry partner, CropPro Consulting [6]. High resolution ground images are collected using a quad mounted camera in a

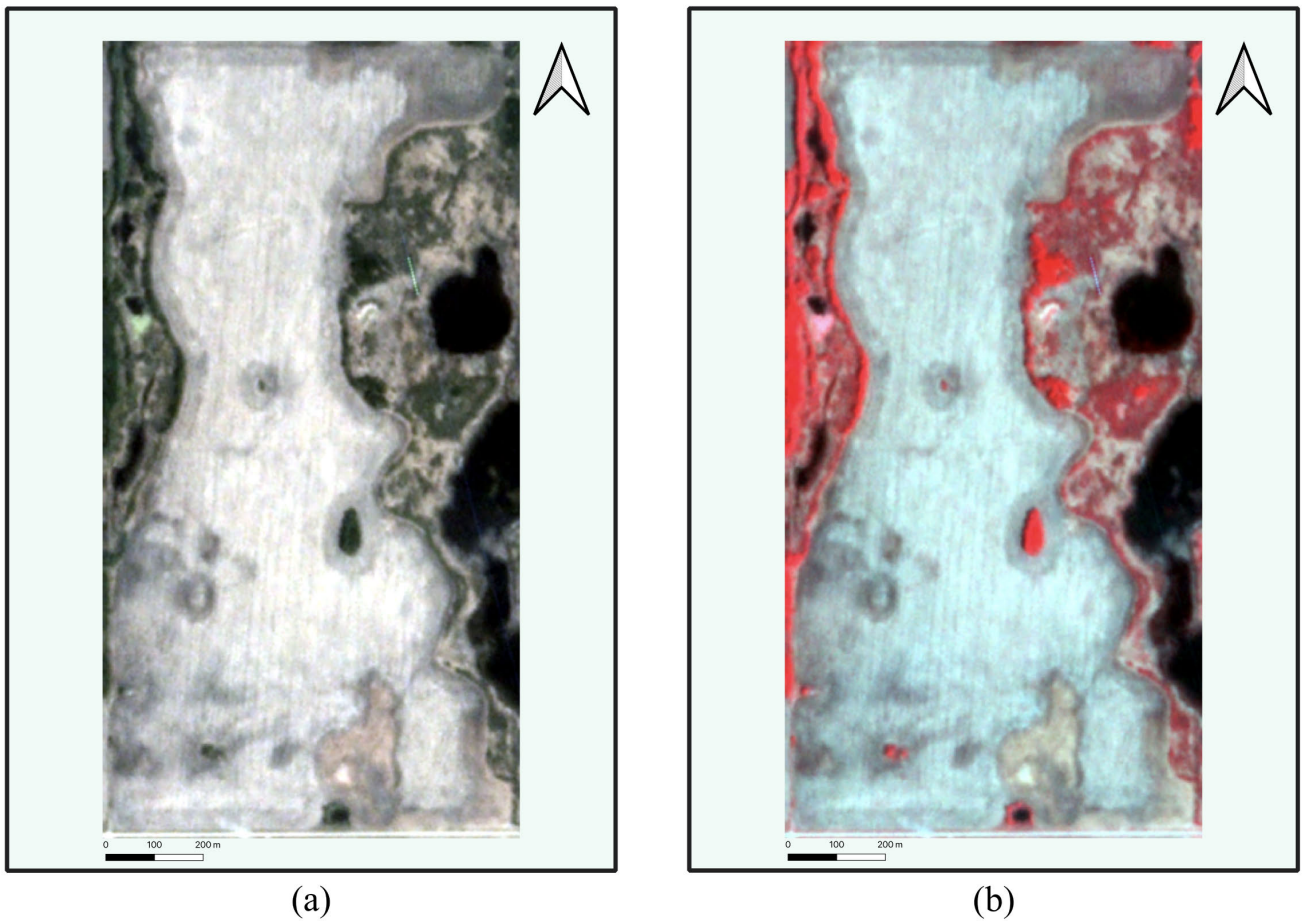

FIGURE 2. Satellite imagery of oats fields: (a) True color composition (b) False color composition [courtesy planet labs inc.]

TABLE 1. Types of weeds.

Fields	Date of Image Acquisition	Image Count
F1	June 3, 2019	600
F2	May 30, 2019	380
F3	June 10, 2019	1091

grid pattern of 80ft by 60ft. The camera is positioned 1m above ground and images are of dimension 1616 × 1080 pixels. A total of 2071 images are collected from the three fields proportionally representing all SWAT zones. Field-1(F1) has very few weeds. Field-2(F2) is moderately weedy and Field-3 (F3) is highly weedy. Images for F1 and F2 are acquired in dry weather resulting in sparse weeds while F3 has high weeds because it is sampled in June 2019 after rain fall. Table 1 summarizes the details of ground image acquisition.

B. SATELLITE IMAGERY

Satellite imagery is taken from RapidEye satellite of Planet Lab Inc. [37]. Four spectral bands blue, green, red, and Near Infrared (NIR) are used. The ground spatial distance of RapidEye is 5 m. An issue with the satellite images is cloud cover. We have selected satellite imagery with less than 5% cloud cover. Other criterion for image selection is the timestamp of satellite imagery. Endeavours are made that the timestamp of satellite imagery closely matches the timestamp of high resolution ground imagery. Fig. 2 shows the example of satellite imagery used in this paper. Fig. 2a is the true color representation of satellite imagery which demonstrates spectral variations. Similarly, Fig. 2b shows false color composition where NIR band is assigned red channel. False color emphasizes the variations in vegetation due to NIR band's sensitivity to chlorophyll.

Vegetation indices are widely employed for estimation of LAI. Apart from growth monitoring, vegetation indices are related to biological properties of plants. Vegetation indices' relationship is non linear with LAI [16]. Therefore, based on RapidEye visual and NIR spectra, we have calculated six vegetation indices: NDVI [38], Green NDVI (GNDVI) [39], Simple Ratio (SR) [40], Enhanced Vegetation Index (EVI) [41], Green Chlorophyll Index (CL-G) [42] and Soil Adjusted Vegetation Index (SAVI) [43] given by following equations. These vegetation indices are related with

LAI variations.

$$NDVI = \frac{(R_{NIR} - R_{Red})}{(R_{NIR} + R_{Red})} \quad (1)$$

$$GNDVI = \frac{(R_{NIR} - R_{Green})}{(R_{NIR} + R_{Green})} \quad (2)$$

$$SR = \frac{R_{NIR}}{R_{Red}} \quad (3)$$

$$EVI = \frac{2.5\,(R_{NIR} - R_{Red})}{(1 + R_{NIR} + 6R_{Red} - 7.5R_{Blue})} \quad (4)$$

$$CL - G = (R_{NIR} - R_{Green}) - 1 \quad (5)$$

$$SAVI = \frac{1.5\,(R_{NIR} - R_{Red})}{(R_{NIR} + R_{Red} + 0.5)} \quad (6)$$

C. SOIL, WATER, AND TOPOGRAPHY MAPS

SWAT map is a single layer map constructed from proximal sensing of the soil. Various proximal sensors measure EC and EV of the land. In addition to EC and EV, WF patterns and accumulations are used to construct single layer SWAT maps [6]. SWAT map divides land into 10 zones. As we move from Zone 1 to Zone 10, topography changes from hills to depressions, low fertile lands give way to saline lands and, water and organic content increases. This soil zoning is helpful in identifying high and low yield potential areas in the field. Currently this soil potential zoning is used for variable rate seeding and fertilizers [44]. In addition to composite SWAT map, we are feeding separate layers of soil properties into the network. These soil maps include EC, EV, and WF of the fields. These maps have a spatial resolution of 8 ft. Fig. 3 refers to normalized SWAT and soil properties map for F3. Red label in map shows minimum value and dark green shows the maximum.

D. DATA PREPROCESSING

Multispectral satellite data, SWAT, and soil properties maps are pre-processed for spatial alignment. First step of spatial alignment is to bring all the maps on a common coordinate system. The second step is to match spatial resolution. Cubic interpolation is used to match resolution of satellite data with SWAT and soil properties map. For radiometric calibration, bit depth of all the maps is set to 16 bits and min-max normalization is used to calibrate pixels on same scale. High resolution RGB images are preprocessed using maximum likelihood classification and semantic segmentation to estimate CLAI and WLAI, which will serve as ground truth labels in the model. Semantic segmentation process is based on our previous work of weed detection and mapping [35], [36].

E. ARTIFICIAL NEURAL NETWORK

ANN is analogous to human brain, which has ability to model complex non-linear relationships. A typical ANN contains a minimum of three layers: input layer, hidden layer and output layer. There could be multiple hidden layers defining the depth of the network. Neurons in the hidden layer forward the input through a non-linear activation function which helps solve non-linear regression and classification problems. In this study, ANN is used to model non-linear relationship of LAIs with vegetation indices, SWAT and soil properties map. ANN with three hidden layers is trained where input to the network is a stack of six vegetation indices, SWAT map, and soil properties maps. At every pixel location, a vector of length 10 is constructed consisting of six vegetation indices, SWAT, EC, EV, and WF. Only those pixel locations are used for training that corresponds to geo-tagged high resolution ground imagery. ANN maps a function between input satellite imagery and soil properties map, and output WLAI and CLAI. Once a model is trained using limited geo-tagged ground imagery then prediction is made for each pixel of the input map. The constructed map using this methodology serves as a basis for prescription by the agronomists. Here, LAI is taken as a use case. Other indicators like plant stand count and individual plant biomass are other use cases. Table 2 summarizes the hyper-parameter settings for the ANN.

TABLE 2. Hyperparameter settings for ANN.

Parameter	Values
Layer1	32
Layer2	64
Dropout Rate	30%
Activation Function	ReLU
Optimizer	Adam
Loss Function	Mean Square Error
Learning Rate	0.001
Batch Size	64
Epochs	10000

IV. RESULTS DISCUSSION AND ANALYSIS

The proposed WLAI and CLAI estimation process is tested on three oat fields. Relationship between LAIs and SWAT zones is established, which is used to estimate distribution of WLAI and CLAI in field as spectra based vegetation indices are not sufficient for bifurcation and distribution of LAIs into WLAI and CALI. Following subsections explain the results for each step of the process.

A. LEAF AREA INDEX AND SWAT ZONES

After segmenting weeds and crops in high resolution ground imagery using semantic segmentation, three types of LAIs are calculated for crop and weed plants. First are CLAI and WLAI of the individual images. It highlights the spatial distribution of weeds and crops over the whole field. Second are average CLAI for each SWAT zone. This parameter emphasis the LAI variations with respect to SWAT zones. Third parameter is patch WLAI which is calculated by averaging the WLAI of images which contain weeds. As weed distribution is not uniform in the field, patch WLAI estimates weed concentration inside weed patches. Patch WLAI helps in deciding the control prescription by agronomist. Average CLAI, Average WLAI and patch WLAIs are estimated using

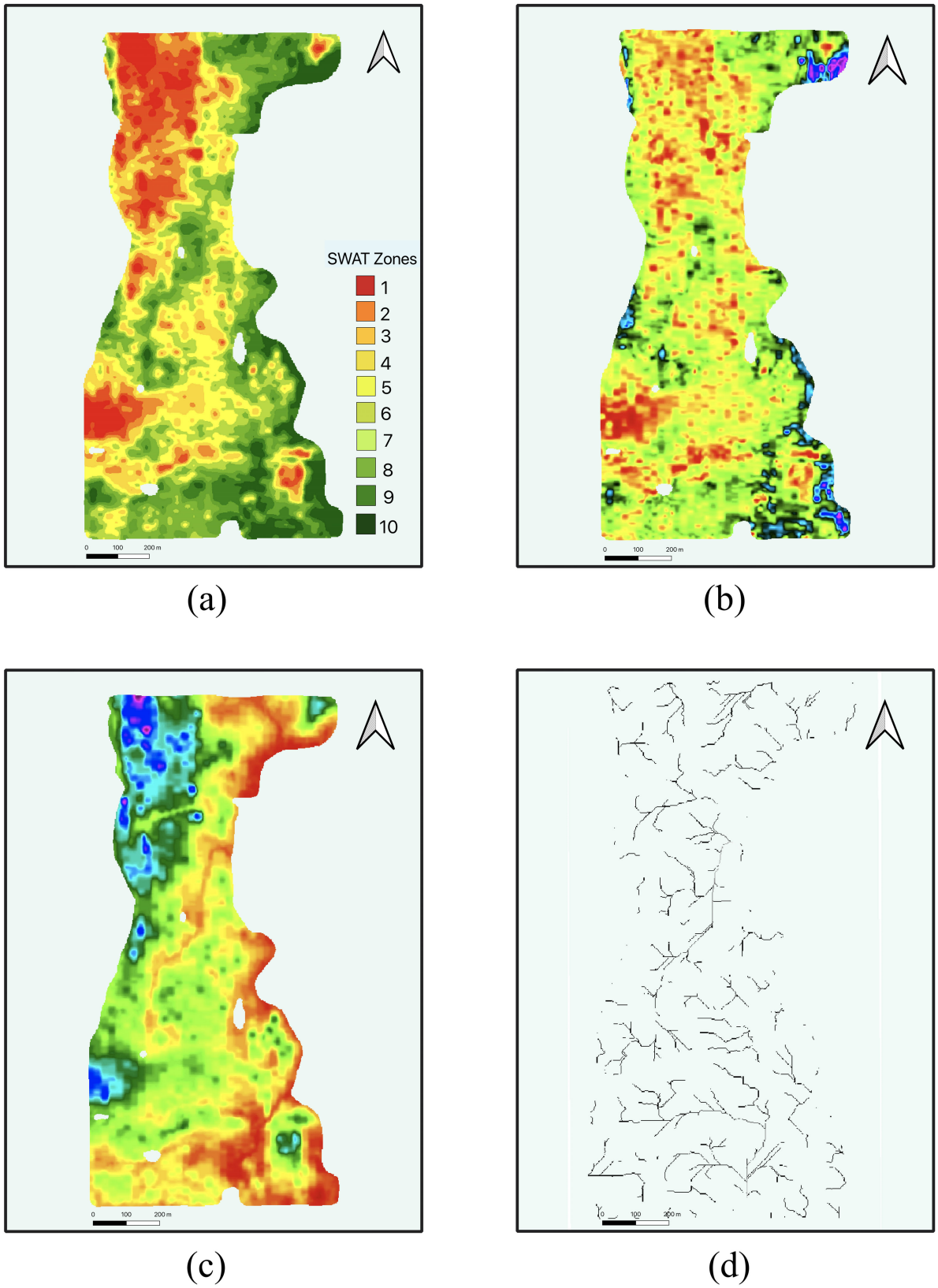

FIGURE 3. (a) SWAT map (b) Electrical conductivity map (c) Elevation map (d) Water flow map [courtesy croppro consulting].

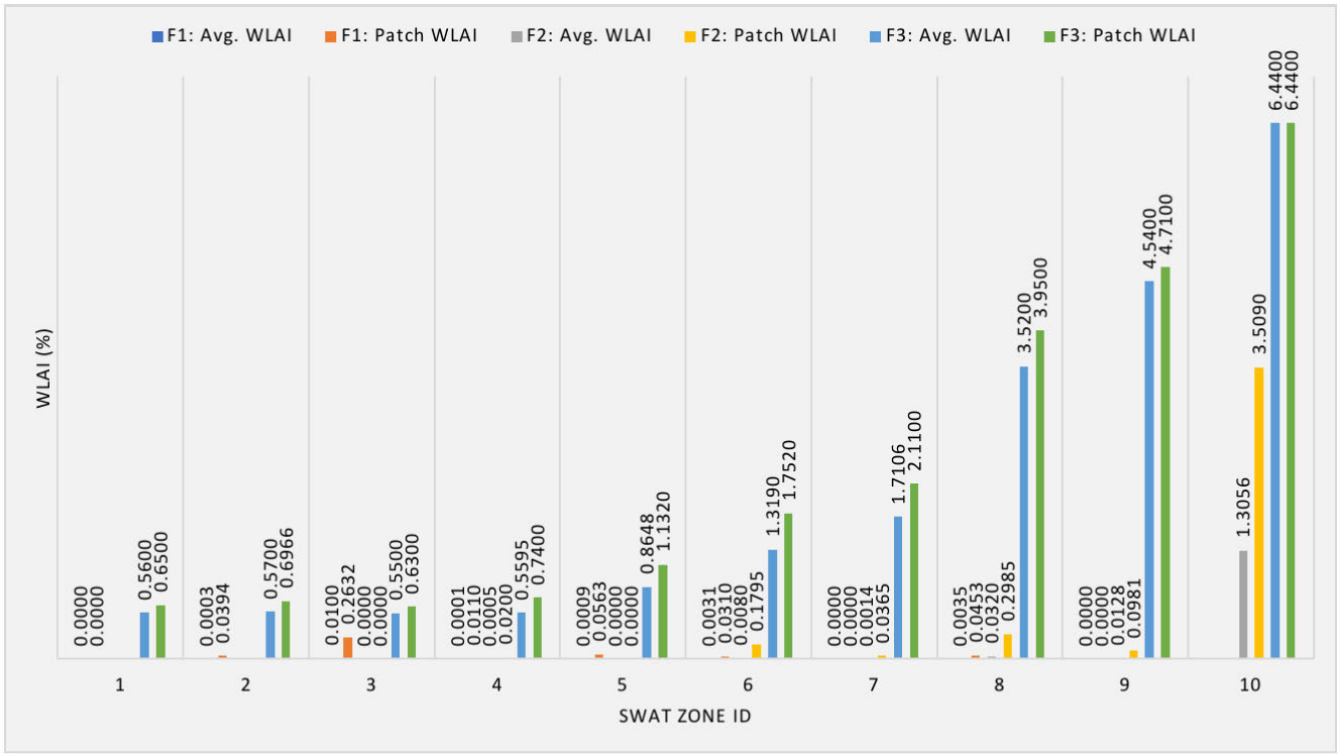

FIGURE 4. Average WLAI and patch WLAI in SWAT zones.

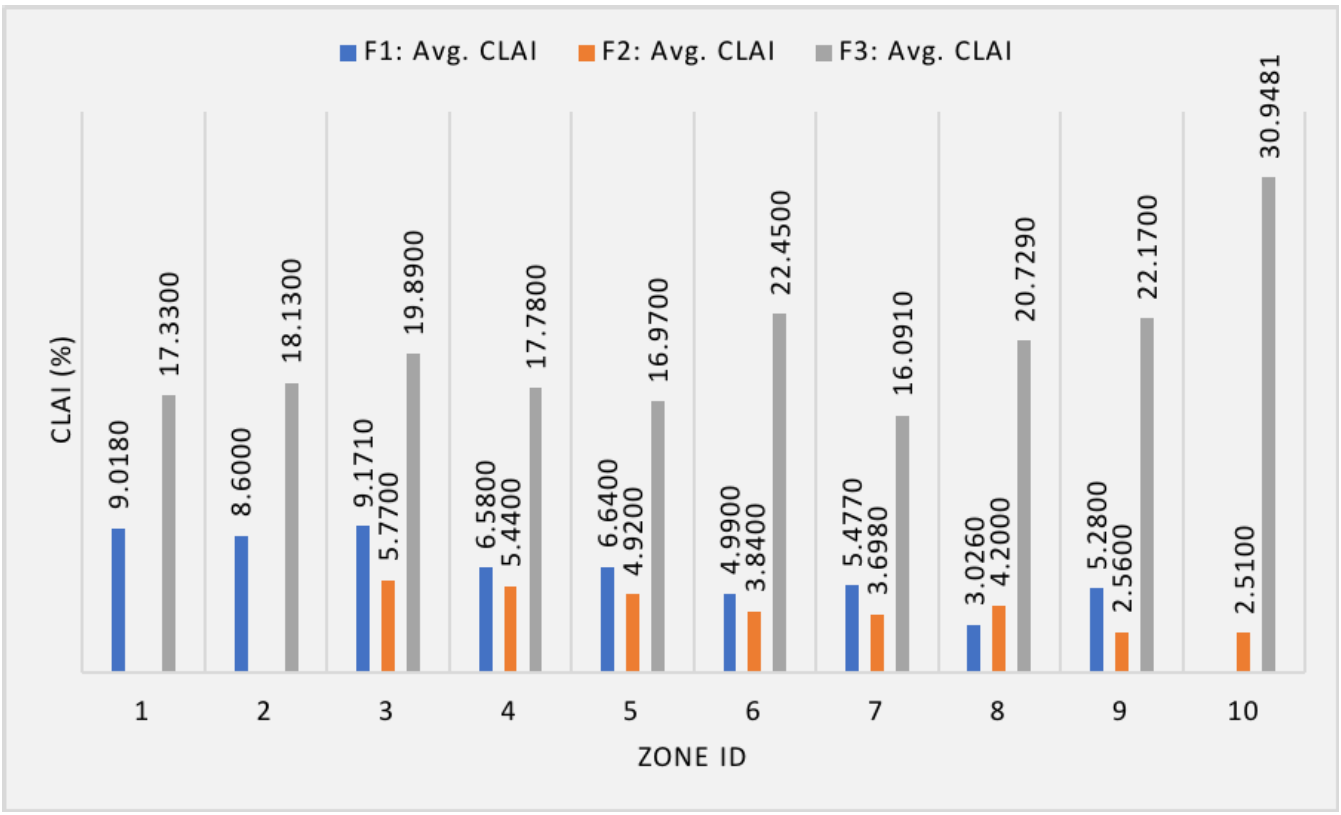

FIGURE 5. Average CLAI and patch CLAI in SWAT zones.

TABLE 3. WLAIs (%) and CLAIs (%) in SWAT zones for oat fields.

	Parameter	SWAT Zone ID									
		1	2	3	4	5	6	7	8	9	10
F1	Avg. WLAI	0	0.00	0.010	0.000	0.001	0.003	0	0.004	0	-
	Patch WLAI	0	0.039	0.263	0.011	0.056	0.031	0	0.045	0	-
	Avg. CLAI	9.018	8.60	9.171	6.58	6.64	4.99	5.477	3.026	5.28	-
F2	Avg. WLAI	-	-	0	0.000	0	0.008	0.001	0.032	0.013	1.306
	Patch WLAI	-	-	0	0.02	0	0.179	0.037	0.299	0.098	3.509
	Avg. CLAI	-	-	5.77	5.44	4.92	3.84	3.698	4.20	2.56	2.51
F3	Avg. WLAI	0.56	0.57	0.55	0.559	0.865	1.319	1.7106	3.52	4.54	6.44
	Patch WLAI	0.65	0.697	0.63	0.74	1.132	1.752	2.11	3.95	4.71	6.44
	Avg. CLAI	17.33	18.13	19.89	17.78	16.97	22.45	16.09	20.73	22.17	30.95

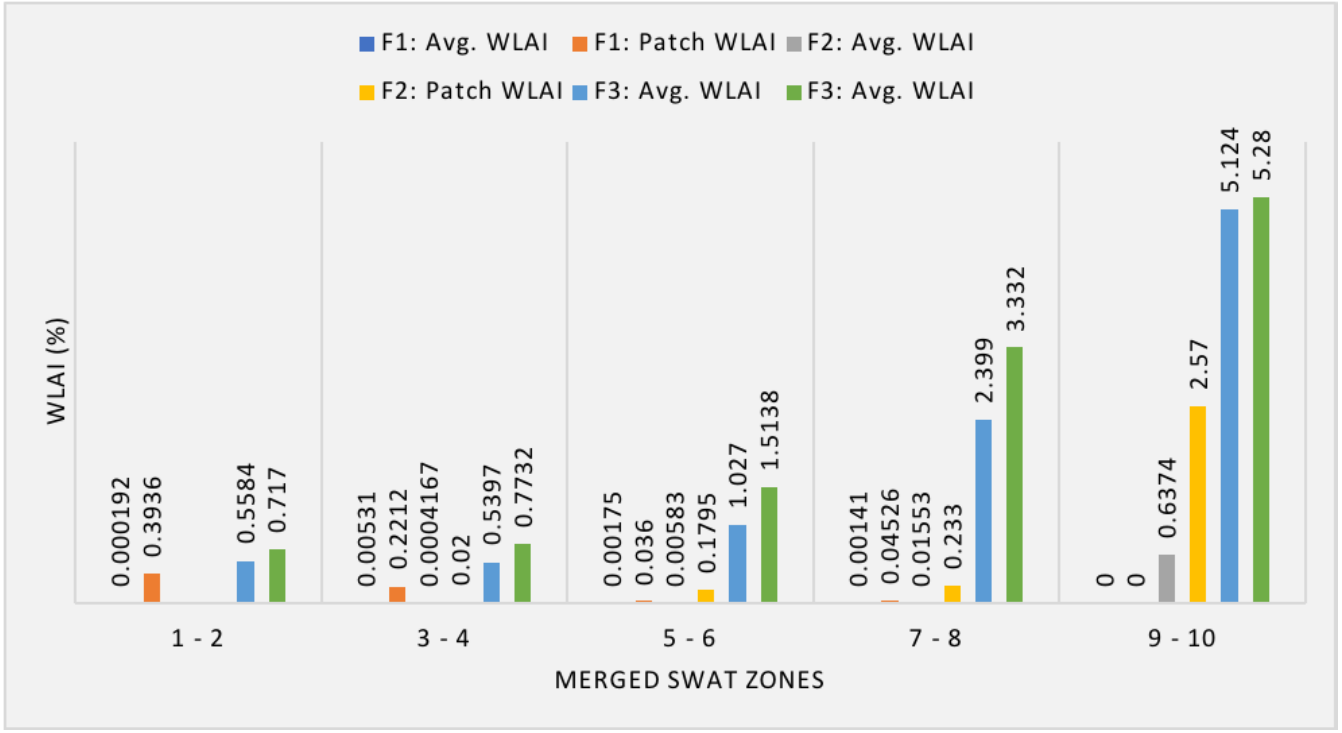

FIGURE 6. Average WLAI and patch WLAI in merged SWAT zones.

following equations:

$$Average\ CLAI = \frac{Crop\ leaf\ pixels\ in\ zone}{Total\ pixels\ in\ zone}$$

$$Average\ WLAI = \frac{Weed\ leaf\ pixels\ in\ zone}{Total\ pixels\ in\ zone}$$

$$Patch\ WLAI = \frac{Weed\ leaf\ pixels\ in\ zone}{Total\ pixels\ of\ images\ with\ weeds\ in\ zone}$$

Fig. 4 plots average WLAI and patch WLAI against SWAT zones for all the three fields. In F1, average WLAI and patch WLAI of SWAT zones indicate that there are few sparse weeds in the field. Also there is no trend observed in F1 with SWAT zone change. F2 does not contain SWAT Zones 1 & 2. Weeds are sparse except in saline zones as evident from low average WLAI parameter. In Zone 6 and onward, average WLAI increases modestly but patch WLAI increases significantly especially in Zone 10. Higher WLAI in Zone 10 is attributed to its characteristic low lying topography and higher organic matter and moisture content. In F3, there are more weed patches and patch WLAI is also higher. There is an increasing trend of WLAI as we move from Zone 1 to Zone 10. In dry Zones 1, 2, 3 & 4, WLAI rise is modest, but as we go beyond Zone 4, WLAI rises sharply. Fig. 5 refers to average CLAI in SWAT zones. In F1 and F2, CLAI decreases modestly from Zone 1 to Zone 10. For F2, CLAI decreases from Zone 1 to Zone 10. CLAI is showing non-linear variations because all understudy fields are applied with variable rate seeding and fertilizers. Variable rate seeding and fertilizers are applied to achieve uniform crop growth irrespective of soil potential. It can also be observed that CLAI and WLAI for F3 are comparatively higher because the data is collected after wet weather conditions. Table 3

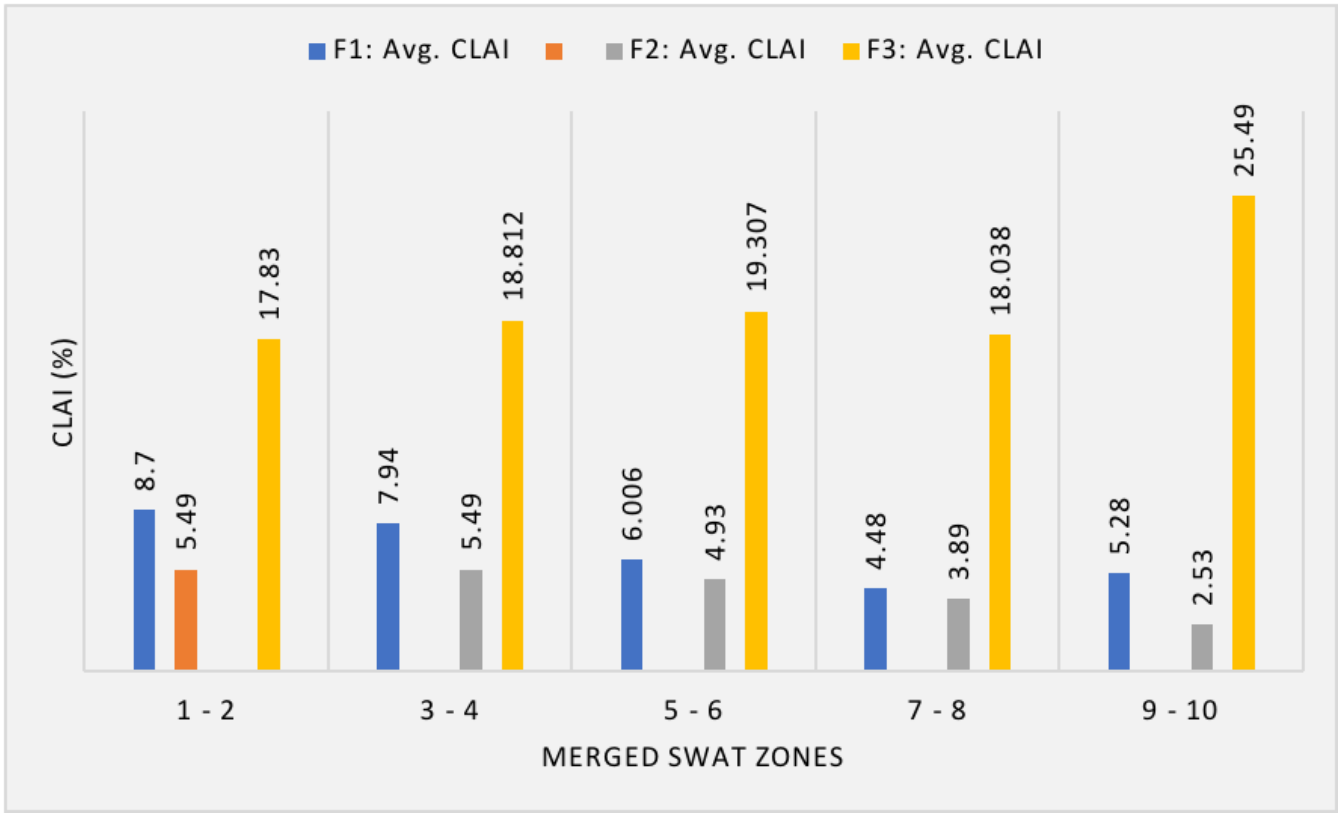

FIGURE 7. Average CLAI and patch CLAI in merged SWAT zones.

summarizes the LAIs for all the three fields in each of the SWAT zones.

As discussed in methodology, originally there are ten zones in the SWAT map. To test if a stronger relationship exists between LAIs and soil properties, we have merged consecutive SWAT zones into five zones. The rationale behind SWAT zone merging is to explore the potential of identifying homogenized management zones for herbicide application as consecutive SWAT zones have similar soil characteristics. Fig. 6 demonstrates the relationship between WLAIs and merged SWAT zones. It is observed that monotonically increasing trend is observed as we move from merged Zones 1 & 2 to 9 &10 for F2 & F3. It means that there exists a strong relationship between WLAIs and merged adjacent SWAT zones except F1. F1 has too few weeds to show any relationship with SWAT zones. Fig. 7 refers to distribution of CLAIs in merged SWAT zones. We can see the CLAIs are more or less consistent across the merged zones. Moderate variations in CLAIs are attributed to the fact that these fields are applied with variable rate seeding and fertilizers. The idea behind variable rate seeding and fertilizers is to achieve uniform consistency of crop establishment and yield across the field. Table 4 summarizes the LAIs with respect to merged SWAT zones.

To quantify the strength of relationship between LAIs, SWAT zones, and soil properties, correlation matrix is calculated as shown in Table 5. It shows that relationship exists between WLAI and CLAI, and SWAT zones, EC, EV, and WF. It can be observed that SWAT relation is stronger with LAIs as compared to separate EC, EV and WF layers.

Table 6 summaries correlation coefficients between average LAIs and patch LAIs, and original and merged SWAT zones. The results demonstrate that LAIs are positively

TABLE 4. WLAIs (%) and CLAIs (%) in merged SWAT zones for oat fields.

	Parameter	SWAT Zone ID				
		1-2	3-4	5-6	7-8	9-10
F-1	Avg. WLAI	0.000	0.005	0.001	0.001	0
	Patch WLAI	0.393	0.221	0.036	0.045	0
	Avg. CLAI	8.7	7.94	6.006	4.48	5.28
F-2	Avg. WLAI	-	0.000	0.006	0.016	0.637
	Patch WLAI	-	0.02	0.179	0.233	2.57
	Avg. CLAI	-	5.49	4.93	3.89	2.53
F-3	Avg. WLAI	0.558	0.539	1.027	2.399	5.124
	Patch WLAI	0.717	0.773	1.513	3.332	5.28
	Avg. CLAI	17.83	18.812	19.307	18.038	25.49

TABLE 5. Correlation matrix of between LAIs, SWAT and soil properties.

	WLAI	CLAI	SWAT	EC	EV	WFP
WLAI	1.0000					
CLAI	0.2729	1.0000				
SWAT	0.4411	0.2014	1.0000			
EC	0.2309	0.2511	0.1131	1.0000		
EV	-0.1657	-0.2074	-0.0213	-0.7719	1.0000	
WFP	0.0181	0.0499	-0.0217	0.0311	-0.0217	1.0000

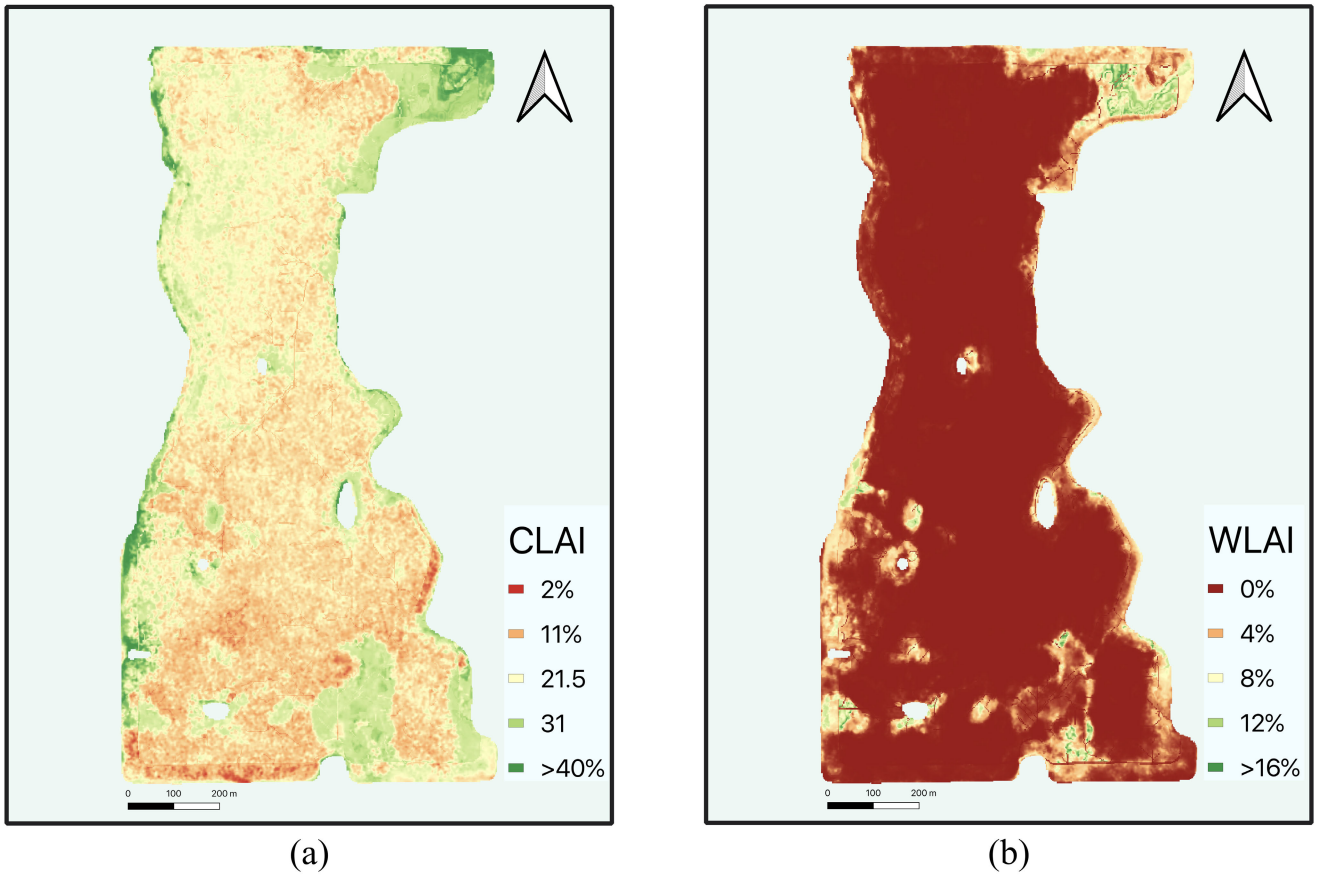

FIGURE 8. Field-3: (a) CLAI Map (b) WLAI Map.

TABLE 6. Correlation coefficients between average LAIs and Patch LAIs, and SWAT zonings.

SWAT Zoning	Parameter	F1	F2	F3
Original SWAT Zones	Avg. WLAI	-0.102	0.590	0.882
	Patch WLAI	-0.269	0.618	0.908
	Avg. CLAI	-0.890	-0.946	0.655
Merged SWAT Zones	Avg. WLAI	-0.317	0.722	0.896
	Patch WLAI	-0.917	0.766	0.942
	Avg. CLAI	-0.913	0.249	0.723

related (taking individual LAIs of each image) with SWAT zones for F2 & F3 though it is a weak relationship. However, average LAIs and average patch WLAI exhibit strong relationship with SWAT zones and it becomes even stronger with the merged zones. In case of F1, small negative correlation between SWAT zones and WLAI shows weak relationship. The weak negative relationship with SWAT zones may be due to two main reasons: Firstly, size of Zones 7-10 is small than Zones 1-6 and secondly, weeds are sparsely distributed in the field.

B. MAPPING LEAF AREA INDEX ON FIELD

In the three selected fields, F3 WLAI has shown strong relationship with SWAT zones. F3 is selected for training a machine learning model to map CLAI and WLAI for the whole field. The ANN proposed in methodology is fed with six vegetation indices, SWAT zoning and soil properties maps. The ground truth LAIs are provided through semantic segmentation as mentioned in methodology section. Two separate ANN models are trained, one for WLAI and other for CLAI. Prior to training, the data is divided into 80%-20% ratio of training and validation data. Models are trained with NVIDIA GPU support. Training and validation Root Mean Square Error (RMSE) of CLAI models are 0.0064 and 0.0096 respectively. Similarly, training and validation RMSE for WLAI are 0.00049 and 0.00058. Loss for WLAI is significantly less than CLAI which means that there is good model fit for WLAI. It also signifies that WLAI is strongly related with model inputs.

Fig. 8 shows the CLAI and WLAI maps constructed through model predictions. It can be observed that CLAI is uniform except at the edges of the field. However, weed distribution is sparse in field and it is mainly concentrated at field edges which are wet and saline zones in SWAT categorization. There are two reasons for it: 1) the control measures for weeds in the wet zones are not as effective as in dry zones and 2) saline and wet zones are highly fertile and supportive for weeds as weeds adapt to soil conditions.

V. CONCLUSION

LAI estimation using direct and remote sensing based methods is widely used to monitor crop growth and health. However bifurcation of LAI into CLAI and WLAI is needed prior to SSM like variable rate herbicides. In addition to this, we also need to know soil related causes of CLAI and WLAI variations for deciding crop prescription. Factors like date of sowing, weather conditions and historical record like herbicides, variable rate seeding and fertilizers also affect in-field distribution of WLAI and CLAI. Consequently there can not be any universal SWAT zone specific prescription for the field. The prescription has to be field specific. Correlational study demonstrates that WLAI is higher in wet, saline and low laying zones while it decreases in dry and high SWAT zones. It means that WLAI estimated from limited high resolution ground imagery using semantic segmentation can be extended to the whole field if SWAT zoning and soil properties are known. In this paper, we have studied this potential of estimating WLAI and CLAI using limited high resolution ground imagery, remote sensing based vegetation indices, SWAT zoning and soil properties for the sake of providing basis for variable rate SSM. Remote sensing based vegetation indices provide the global information about the biological characteristics of vegetation, and SWAT / soil maps provide information regarding soil related causes of CLAI and WLAI variations. Our results demonstrate that limited high resolution ground imagery, vegetation indices and SWAT / soil maps can be used to model CLAI and WLAI.

ACKNOWLEDGMENT

The authors would like to thank CropPro Consulting (www.croppro.ca) for providing them with high-resolution images and SWAT maps. They acknowledge Planet Lab's support in providing them with high resolution satellite imagery.

REFERENCES

[1] P. Chivenge and S. Sharma, "Precision agriculture in food production: Nutrient management," in *Proc. Int. Conf. ICTs Precis. Agricult.*, 2019, p. 12.

[2] R. E. Plant, "Site-specific management: The application of information technology to crop production," *Comput. Electron. Agricult.*, vol. 30, nos. 1–3, pp. 9–29, Feb. 2001.

[3] P. S. Thenkabail, J. G. Lyon, and A. Huete, *Advanced Applications in Remote Sensing of Agricultural Crops and Natural Vegetation*. Boca Raton, FL, USA: CRC Press, 2018.

[4] A. Viña, A. A. Gitelson, A. L. Nguy-Robertson, and Y. Peng, "Comparison of different vegetation indices for the remote assessment of green leaf area index of crops," *Remote Sens. Environ.*, vol. 115, no. 12, pp. 3468–3478, Dec. 2011.

[5] C. Atzberger, "Advances in remote sensing of agriculture: Context description, existing operational monitoring systems and major information needs," *Remote Sens.*, vol. 5, no. 2, pp. 949–981, Feb. 2013.

[6] CropPro Consulting. (2020). *What is SWAT Map?*. Accessed: Jun. 18, 2020. [Online]. Available: https://www.swatmaps.com/swat-maps

[7] N. J. J. Breda, "Ground-based measurements of leaf area index: A review of methods, instruments and current controversies," *J. Experim. Botany*, vol. 54, no. 392, pp. 2403–2417, Sep. 2003.

[8] T. N. Carlson and D. A. Ripley, "On the relation between NDVI, fractional vegetation cover, and leaf area index," *Remote Sens. Environ.*, vol. 62, no. 3, pp. 241–252, Dec. 1997.

[9] T. Dong, J. Liu, J. Shang, B. Qian, B. Ma, J. M. Kovacs, D. Walters, X. Jiao, X. Geng, and Y. Shi, "Assessment of red-edge vegetation indices for crop leaf area index estimation," *Remote Sens. Environ.*, vol. 222, pp. 133–143, Mar. 2019.

[10] M. S. Mkhabela, P. Bullock, S. Raj, S. Wang, and Y. Yang, "Crop yield forecasting on the Canadian prairies using MODIS NDVI data," *Agricult. Forest Meteorol.*, vol. 151, no. 3, pp. 385–393, Mar. 2011.

[11] A. L. Nguy-Robertson, Y. Peng, A. A. Gitelson, T. J. Arkebauer, A. Pimstein, I. Herrmann, A. Karnieli, D. C. Rundquist, and D. J. Bonfil, "Estimating green LAI in four crops: Potential of determining optimal spectral bands for a universal algorithm," *Agricult. Forest Meteorol.*, vols. 192–193, pp. 140–148, Jul. 2014.

[12] A. Kross, H. McNairn, D. Lapen, M. Sunohara, and C. Champagne, "Assessment of RapidEye vegetation indices for estimation of leaf area index and biomass in corn and soybean crops," *Int. J. Appl. Earth Observ. Geoinf.*, vol. 34, pp. 235–248, Feb. 2015.

[13] J. Shang, H. McNairn, U. Schulthess, R. Fernandes, and J. Storie, "Estimation of crop ground cover and leaf area index (LAI) of wheat using RapidEye satellite data: Prelimary study," in *Proc. 1st Int. Conf. Agro-Geoinform. (Agro-Geoinformatics)*, Aug. 2012, pp. 1–5.

[14] M. Hosseini, H. McNairn, S. Mitchell, L. Dingle Robertson, A. Davidson, and S. Homayouni, "Synthetic aperture radar and optical satellite data for estimating the biomass of corn," *Int. J. Appl. Earth Observ. Geoinf.*, vol. 83, Nov. 2019, Art. no. 101933.

[15] L. Wang, X. Zhou, X. Zhu, Z. Dong, and W. Guo, "Estimation of biomass in wheat using random forest regression algorithm and remote sensing data," *Crop J.*, vol. 4, no. 3, pp. 212–219, Jun. 2016.

[16] O. Reisi Gahrouei, H. McNairn, M. Hosseini, and S. Homayouni, "Estimation of crop biomass and leaf area index from multitemporal and multispectral imagery using machine learning approaches," *Can. J. Remote Sens.*, vol. 46, no. 1, pp. 84–99, Jan. 2020.

[17] J. Martínez-Guanter, G. Egea, M. Pérez-Ruiz, and O. Apolo-Apolo, "Estimation of the leaf area index in maize based on UAV imagery using deep learning techniques," in *Precision Agriculture*. Wageningen, The Netherlands: Academic, 2019, p. 1304.

[18] R. Ferguson and D. Rundquist, "Remote sensing for site-specific crop management," in *Precision Agriculture Basics*. Madison, WI, USA: American Society of Agronomy, Crop Science Society of America, and Soil, 2018, pp. 103–118.

[19] D. R. Ess, M. T. Morgan, and S. Parson, "Implementing site-specific management: Map-versus sensor-based variable rate application," Site-Specific Manage. Center, Purdue Univ., West Lafayette, IN, USA, Tech. Rep. SSM-2-W, 2001.

[20] I. Bolat and M. Öztürk, "Effects of altitudinal gradients on leaf area index, soil microbial biomass c and microbial activity in a temperate mixed forest ecosystem of northwestern Turkey," *iForest-Biogeosci. Forestry*, vol. 10, no. 1, p. 334, 2016.

[21] H. Liang, K. Hu, W. Qin, Q. Zuo, and Y. Zhang, "Modelling the effect of mulching on soil heat transfer, water movement and crop growth for ground cover rice production system," *Field Crops Res.*, vol. 201, pp. 97–107, Feb. 2017.

[22] A. M. Walter, S. Christensen, and S. E. Simmelsgaard, "Spatial correlation between weed species densities and soil properties," *Weed Res.*, vol. 42, no. 1, pp. 26–38, Feb. 2002.

[23] R. Erviö, S. Hyvärinen, L.-R. Erviö, and J. Salonen, "Soil properties affecting weed distribution in spring cereal and vegetable fields," *Agricult. Food Sci.*, vol. 3, no. 5, pp. 497–504, Sep. 1994.

[24] C. Andreasen, J. C. Streibig, and H. Haas, "Soil properties affecting the distribution of 37 weed species in danish fields," *Weed Res.*, vol. 31, no. 4, pp. 181–187, Aug. 1991.

[25] H. Metcalfe, A. E. Milne, R. Webster, R. M. Lark, A. J. Murdoch, and J. Storkey, "Designing a sampling scheme to reveal correlations between weeds and soil properties at multiple spatial scales," *Weed Res.*, vol. 56, no. 1, pp. 1–13, Feb. 2016.

[26] H. Metcalfe, A. E. Milne, R. Hull, A. J. Murdoch, and J. Storkey, "The implications of spatially variable pre-emergence herbicide efficacy for weed management," *Pest Manage. Sci.*, vol. 74, no. 3, pp. 755–765, Mar. 2018.

[27] Z. Mavunganidze, I. C. Madakadze, J. Nyamangara, and P. Mafongoya, "Influence of selected soil properties, soil management practices and socio-economic variables on relative weed density in a hand hoe-based conservation agriculture system," *Soil Use Manage.*, vol. 32, no. 3, pp. 433–445, Sep. 2016.

[28] H. Metcalfe, A. E. Milne, A. J. Murdoch, and J. Storkey, "Does variable soil pH have an effect on the within-field distribution of A. Myosuroides?" in *Crop Production in Southern Britain*, R. I. C. Hull, G. Jellis, M. May, P. Miller, S. R. Moss, C. Nicholls, and J. Orson, Eds. Wellesbourne, U.K.: Association of Applied Biologists, 2017. [Online]. Available: https://repository.rothamsted.ac.uk/item/8w167/does-variable-soil-ph-have-an-effect-on-the-within-field-distribution-of-a-myosuroides
[29] N. E. Korres, J. K. Norsworthy, K. R. Brye, V. Skinner, Jr., and A. Mauromoustakos, "Relationships between soil properties and the occurrence of the most agronomically important weed species in the field margins of eastern Arkansas–implications for weed management in field margins," *Weed Res.*, vol. 57, no. 3, pp. 159–171, Jun. 2017.
[30] H. Metcalfe, A. E. Milne, K. Coleman, A. J. Murdoch, and J. Storkey, "Modelling the effect of spatially variable soil properties on the distribution of weeds," *Ecol. Model.*, vol. 396, pp. 1–11, Mar. 2019.
[31] C. Georgi, D. Spengler, S. Itzerott, and B. Kleinschmit, "Automatic delineation algorithm for site-specific management zones based on satellite remote sensing data," *Precis. Agricult.*, vol. 19, no. 4, pp. 684–707, Aug. 2018.
[32] J. Behmann, A.-K. Mahlein, T. Rumpf, C. Römer, and L. Plümer, "A review of advanced machine learning methods for the detection of biotic stress in precision crop protection," *Precis. Agricult.*, vol. 16, no. 3, pp. 239–260, Jun. 2015.
[33] K. Liakos, P. Busato, D. Moshou, S. Pearson, and D. Bochtis, "Machine learning in agriculture: A review," *Sensors*, vol. 18, no. 8, p. 2674, Aug. 2018.
[34] A. Kamilaris and F. X. Prenafeta-Boldú, "A review of the use of convolutional neural networks in agriculture," *J. Agricult. Sci.*, vol. 156, no. 3, pp. 312–322, Apr. 2018.
[35] M. H. Asad and A. Bais, "Weed detection in canola fields using maximum likelihood classification and deep convolutional neural network," *Inf. Process. Agricult.*, to be published, doi: 10.1016/j.inpa.2019.12.002.
[36] M. H. Asad and A. Bais, "Weed density estimation using semantic segmentation," in *Image and Video Technology* (Lecture Notes in Computer Science), vol. 11994. Cham, Switzerland: Springer, 2020, pp. 162–171.
[37] Planet Labs. (2020). *Planer Labs HomePage*. Accessed: Jun. 18, 2020. [Online]. Available: https://www.planet.com
[38] J. W. Rouse, Jr., R. H. Haas, J. Schell, and D. Deering, "Monitoring the vernal advancement and retrogradation (green wave effect) of natural vegetation," Remote Sensing Centre, Texas A & M Univ., College Station, TX, USA, Tech. Rep. 7, 1973.
[39] A. A. Gitelson, Y. J. Kaufman, and M. N. Merzlyak, "Use of a green channel in remote sensing of global vegetation from EOS-MODIS," *Remote Sens. Environ.*, vol. 58, no. 3, pp. 289–298, Dec. 1996.
[40] C. F. Jordan, "Derivation of leaf-area index from quality of light on the forest floor," *Ecology*, vol. 50, no. 4, pp. 663–666, Jul. 1969.
[41] A. Huete, H. Liu, K. Batchily, and W. Leeuwen, "A comparison of vegetation indices over a global set of TM images for EOS-MODIS," *Remote Sens. Environ.*, vol. 59, no. 3, pp. 440–451, Mar. 1997.
[42] A. A. Gitelson, A. Viña, T. J. Arkebauer, D. C. Rundquist, G. Keydan, and B. Leavitt, "Remote estimation of leaf area index and green leaf biomass in maize canopies," *Geophys. Res. Lett.*, vol. 30, no. 5, pp. n/a–n/a, Mar. 2003.
[43] A. R. Huete, "A soil-adjusted vegetation index (SAVI)," *Remote Sens. Environ.*, vol. 25, no. 3, pp. 295–309, Aug. 1988.
[44] C. Willness. (2018). *SWAT MAPS Making Variable Rate Great Again*. Accessed: Jun. 18, 2020. [Online]. Available: https://farmsmartconference.files.wordpress.com/2018/02/18fs1243-cory-willness-soil-water-and-topography-swat-the-maps-to-variable-rate-success.pdf

MUHAMMAD HAMZA ASAD received the B.Sc. degree in electrical engineering from the University of Engineering and Technology, Lahore, Pakistan, in 2009, and the M.A.Sc. degree in electronic systems engineering from the University of Regina, SK, Canada, in 2019, where he is currently pursuing the Ph.D. degree in electronic systems engineering. His research interests include signal processing, machine learning, computer vision, and artificial intelligence algorithms, with a special focus on precision agriculture and predictive maintenance. He is currently working on site specific biotic and abiotic stress management.

ABDUL BAIS (Senior Member, IEEE) received the M.Sc. degree in electrical engineering from the University of Engineering and Technology, Peshawar, Pakistan, in 2003, and the Ph.D. degree in electrical engineering and information technology from the Vienna University of Technology, Vienna, Austria, in 2007.

From 2010 to 2013, he was a Postdoctoral Fellow with the Faculty of Engineering and Applied Science, University of Regina, SK, Canada, where he has been an Assistant Professor with the Electronic Systems Engineering Program, since 2015. He is a coauthor of 64 peer-reviewed articles. His research interests include real-time data stream mining, deep learning, signal processing, image processing, and computer vision. He is a Certified Instructor with the NVIDIA Deep Learning Institute (Fundamentals of Deep Learning for Computer Vision and Fundamentals of Deep Learning for Multiple Data Types). He is a Licensed Professional Engineer in SK, Canada.